A COMPARATIVE STUDY OF THE COOLING PERFORMANCE OF NEW HVAC SYSTEMS BASED ON THE REVERSED AIR CYCLE

C. CIANFRINI[1], M. CORCIONE[1], A. D'ORAZIO[2] & L. FONTANA[1]
[1]Dipartimento di Fisica Tecnica, University of Rome "La Sapienza", Italy.
[2]Dipartimento di Meccanica e Aeronautica, University of Rome "La Sapienza", Italy.

ABSTRACT

A numerical study on the cooling performance of new air-conditioning systems based on the reversed air cycle is conducted through a specifically developed computer code. The main peculiarity of such HVAC systems is the combination of the roles traditionally played separately by the chiller and the air handling unit, as the expanded cool air is directly supplied to the indoor ambient for its environmental control. For any system proposed, simulations have been carried out for a wide variety of psychrometric states of both outdoor air and supply air, and for different efficiencies of the heat exchangers and the turbomachinery. Among the main results obtained, it is found that for hot and dry climates, as well as for temperate climates, the values of the cooling performance of the most advanced configurations are of the same order as those typical for traditional HVAC systems served by vapour-compression refrigerating units.

Keywords: air-conditioning, innovative integrated systems, numerical simulations, reversed Brayton cycle.

1 INTRODUCTION

The protection of our planet is one of the basic conditions necessary to ensure a really sustainable development for next generations. As known, one of the many related initiatives is the elimination of the environmentally detrimental chemical refrigerants currently in use, and their replacement with environmentally compatible fluids, as stated in the Montreal and Kyoto Protocols.

In this perspective, besides encouraging research on new harmless chemical fluids, on which most of the hopes are placed, it also seems appropriate to make all possible attempts to revive the potential merits of natural refrigerants, beginning from air, which is certainly the most attractive in terms of environmental compatibility, cost and availability [1–6].

Unfortunately, the air-refrigeration operating cycle, i.e. the reversed Brayton cycle, has the disadvantage of large temperature variations of the fluid during the heat-addition and heat-removal processes, which implies that the coefficient of performance of this cycle is considerably lower than that of the corresponding reversed Carnot cycle. Such modest cooling performance of the reversed Brayton cycle may actually be assumed as the main reason for the rather limited use of air-cycle units for air-conditioning purposes, on which our attention is focused. Typical exceptions are represented by aircraft applications [7], where compressed air is available from the jet engines, and lightweight, compact size, high reliability and easy maintenance are considered more important than fuel economy, as well as by some stationary applications where energetic efficiency is not the primary factor, e.g. remotely located, temporary military bases, where portable units may be used. However, such specialized applications lie outside our interests, which are instead focused on residential and commercial building applications.

Indeed, non-negligible increases in the cooling performance may be obtained by the adoption of so called 'integrated HVAC systems'. These are innovative systems which combine the two roles traditionally played separately by the chiller and the air handling unit, as the expanded cool air is supplied directly to the indoor ambient for its environmental control [8, 9].

ISSN: 1743-7601 (paper format), ISSN: 1743-761X (online), http://journals.witpress.com
DOI: 10.2495/SDP-V2-N4-490-509

In this framework, the present paper has a threefold purpose, namely (1) to highlight the main features of the more conventional HVAC systems based on the reversed Brayton cycle; (2) to discuss the main features of several basic and enhanced configurations of such innovative 'integrated HVAC systems' based on the reversed Brayton cycle; and (3) to calculate the cooling performance of the air-conditioning systems considered for a wide variety of combinations of the main governing parameters.

2 HVAC SYSTEMS BASED ON THE REVERSED BRAYTON CYCLE

The main features of both conventional and integrated HVAC systems based on the reversed Brayton cycle are discussed in the following three subsections.

2.1 Conventional HVAC systems

Conventional HVAC systems based on the reversed Brayton cycle may be arranged according to different configurations, whose common feature is the use of expanded refrigerated air for the cooling and dehumidification of outdoor air which has to be supplied to the indoor ambient for its hygrothermal control. The four configurations sketched in Figs 1–4, denoted as CS1, CS2, CS3, and CS4, respectively, are considered. Each of them consists mainly of: (1) an air-cycle machine combining a turbine wheel (T), a driving motor (M) and a rotary compressor (C) on a single shaft; (2) a counterflow, air-to-air, plate heat exchanger (HEC) for cooling and dehumidification of outdoor air; and (3) a re-heating coil (RHC), operated by an indoor ambient temperature controller. Other components are one or two additional counterflow, air-to-air, plate heat exchangers for energy recovery from the exhaust airstream (REC) and/or rejection of the heat of compression above the atmospheric pressure (HCR).

2.2 Basic 'integrated HVAC systems'

Two basic integrated HVAC systems, which share the main characteristic of the 'direct' use of the expanded cool air as supply air, named BIS1 and BIS2, sketched in Figs 5 and 6, respectively, are considered. They consist mainly of: (1) an air-cycle refrigeration machine equipped with a water separator (WS) at the turbine wheel discharge for condensate removal from supply air; (2) a counterflow, air-to-air, plate heat exchanger (REC) in which outdoor air is first subjected to a cooling treatment at atmospheric pressure by heat transfer to exhaust air; (3) a counterflow, air-to-air, plate heat exchanger (HCR) for rejection of the heat of compression either to outdoor air (in system BIS1) or to exhaust air which leaves the recovery equipment (REC) (in system BIS2); and (4) a re-heating coil (RHC) for temperature control of supply air.

2.3 Enhanced 'integrated HVAC systems'

With respect to the basic configurations discussed above, the enhanced configurations distinguish themselves for a rational use of the airstreams available at low temperature for rejection of the heat of compression, and for use of evaporative cooling treatments of the cool airstreams either before the inlet of the air-to-air heat exchangers or along the entire length of the heat exchangers, when applicable. Three enhanced integrated HVAC systems, denoted as EIS1, EIS2 and EIS3, are considered.

Configuration EIS1, sketched in Fig. 7, consists mainly of: (1) an air-cycle refrigeration machine equipped with a water separator (WS) at its outlet; (2) three counterflow, air-to-air, plate heat exchangers (HE1, HE2 and HE3), each one served by an air washer humidifier (AW) at the cool

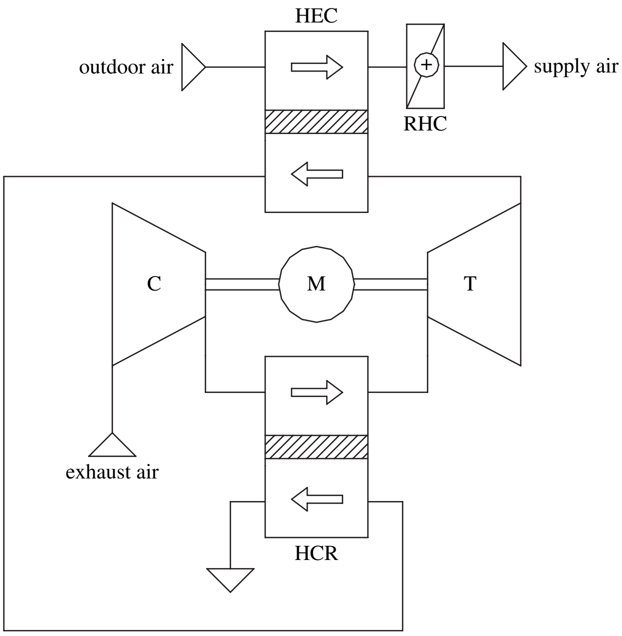

Figure 1: Conventional configuration CS1.

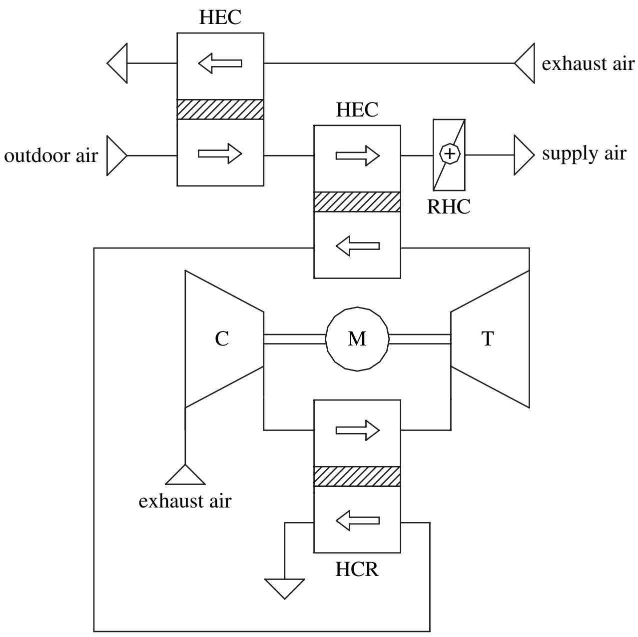

Figure 2: Conventional configuration CS2.

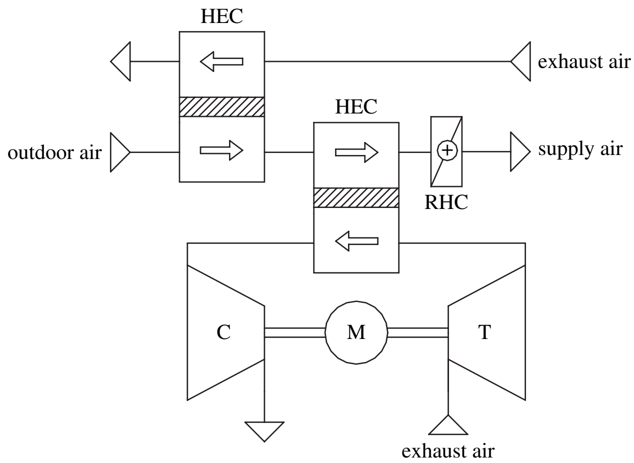

Figure 3: Conventional configuration CS3.

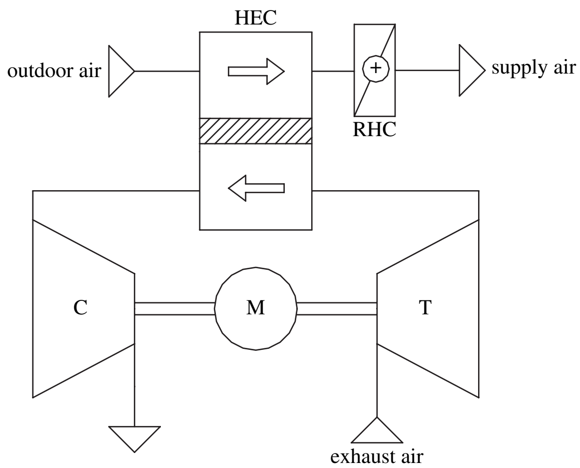

Figure 4: Conventional configuration CS4.

airstream inlet; (3) a system of coupled dampers (CD1), located at the cool airstream inlet of heat exchanger HE2; and (4) a re-heating coil (RHC) for temperature control of supply air. As far as its working principle is concerned, a brief description is given. Outdoor air at atmospheric pressure is first subjected to a cooling treatment in HE1, where heat is transferred to saturated outdoor air, and then compressed in C. The heat of compression is rejected subsequently: (1) in HE2, to saturated air coming from either the outside or the outlet of heat exchanger HE3, according to the position of coupled dampers CD1 operated by controller C1 on the basis of the smaller specific enthalpy (denoted as *j*); and (2) in HE3, to saturated exhaust air. Outdoor air at the upper pressure leaving heat

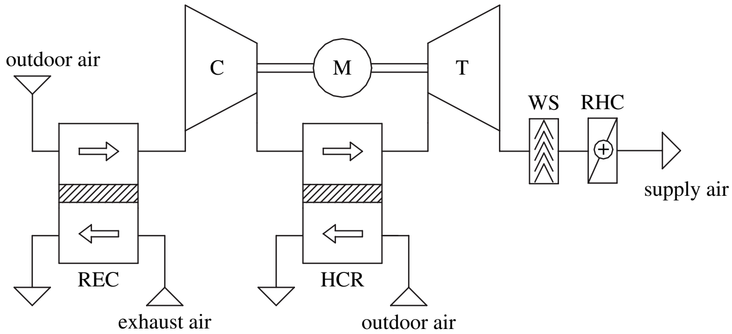

Figure 5: Basic integrated configuration BIS1.

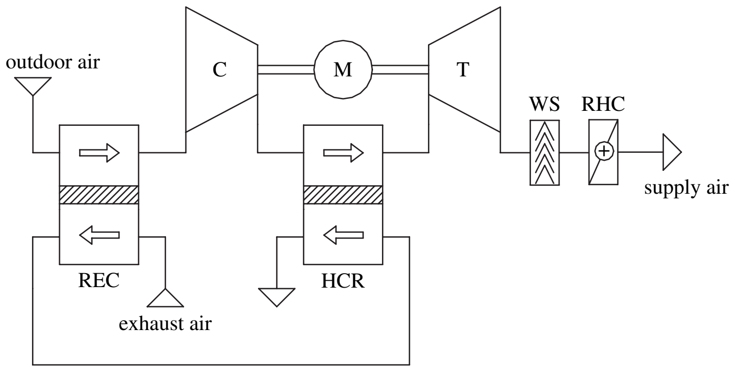

Figure 6: Basic integrated configuration BIS2.

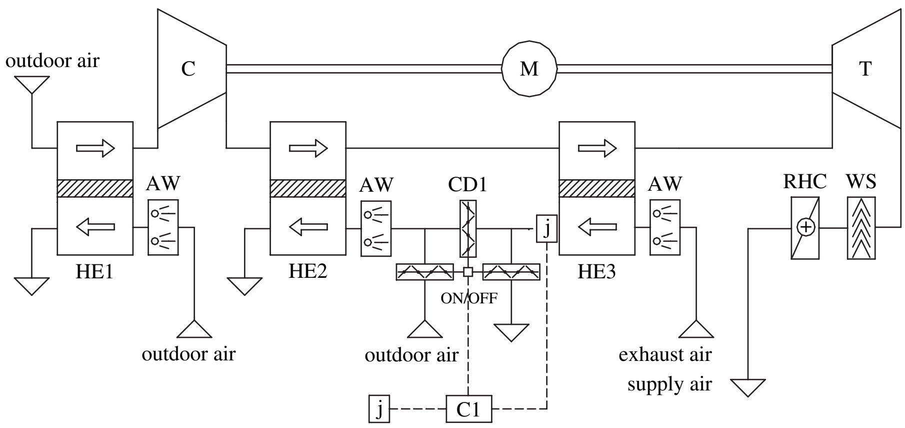

Figure 7: Enhanced integrated configuration EIS1.

exchanger HE3 is finally expanded in T up to atmospheric pressure, with a consequent reduction of its temperature and humidity ratio. A re-heating of supply air may then occur in RHC, when required.

Configuration EIS2, sketched in Fig. 8, is an upgrading of configuration EIS1, from which it is derived by simply adding a further counterflow, air-to-air, plate heat exchanger (HE4) and a further system of coupled dampers (CD2). With respect to configuration EIS1, the heat of compression is rejected subsequently not only in HE2 and HE3, as described above, but also in HE4 to cool air which is discharged by the turbine wheel (T) at the moisture content required for indoor humidity comfort conditions, whenever a re-heating process of the supply air is required. The position of coupled dampers CD2 is modulated by controller C2 according to the indoor air temperature. When the by-pass damper is completely closed, C2 operates on the additional re-heating coil (RHC).

Configuration EIS3, sketched in Fig. 9, represents a further upgrading. Configuration EIS3 is derived directly from configuration EIS2 by assuming that HE1, HE2 and HE3 are wet-surface type

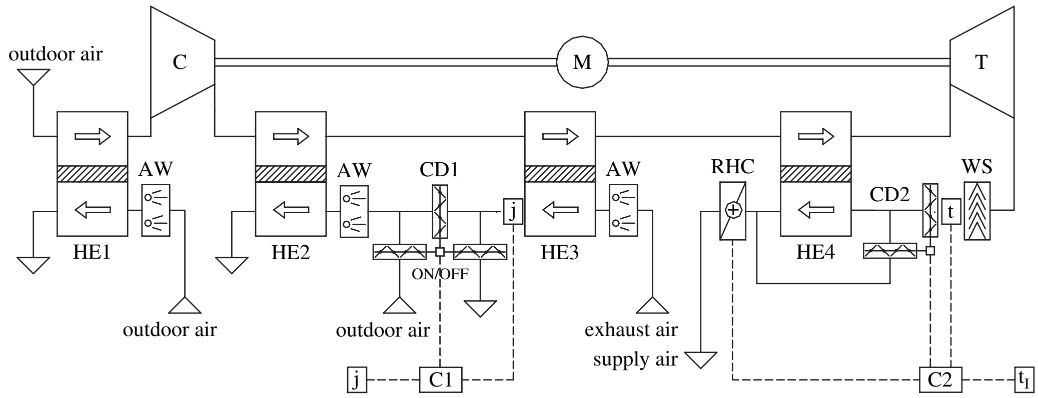

Figure 8: Enhanced integrated configuration EIS2.

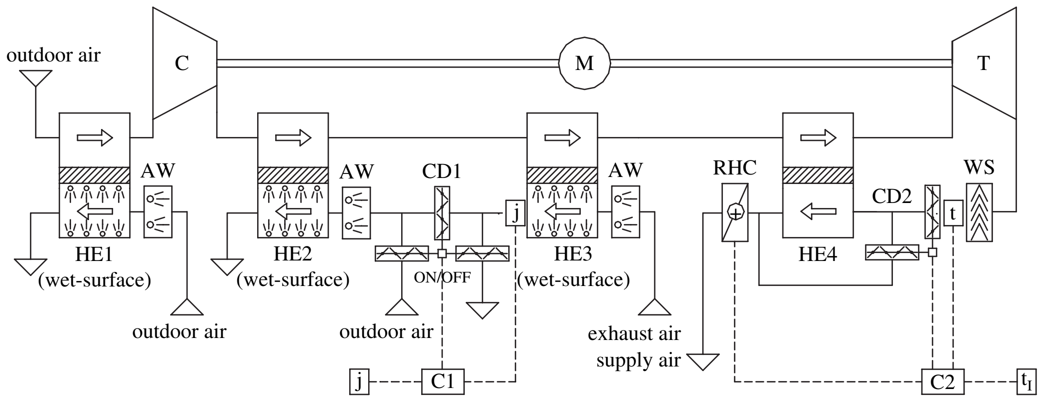

Figure 9: Enhanced integrated configuration EIS3.

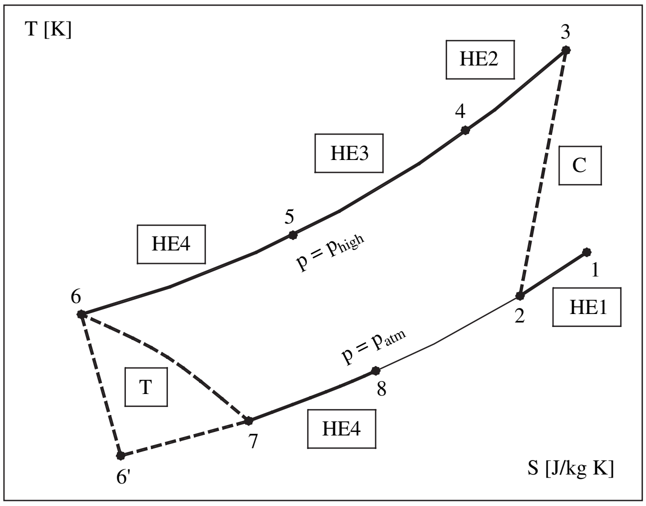

Figure 10: Operating cycle for configurations EIS2 and EIS3.

heat exchangers, i.e. with the boundary surfaces of the cool airstream passages wet by a film of water, whose evaporation enhances the heat transfer effectiveness [10–14].

The operating cycle for configurations EIS2 and EIS3 in the *T–S* diagram is drawn in Fig. 10 under the assumption that the frictional pressure drops through the heat exchangers are negligible, and that the expansion process may be modelled according to a two-stage process, as described in Section 3.1 (in the diagram, each transformation is labelled according to the component in which it occurs).

3 MATHEMATICAL MODEL FOR COOLING PERFORMANCE EVALUATION

The cooling performance of any HVAC system described above is calculated by a specifically developed computer code which simulates the thermodynamic behaviour of each component of the air-conditioning system as described below.

3.1 Turbomachinery

The compression process, assumed as occurring at constant humidity ratio with no stray heat transfer to the surroundings, leads to the following outlet air temperature T_c:

$$T_c = T_{in}\left[\frac{\beta_c^{(\gamma-1)/\gamma} - 1}{\eta_c} + 1\right], \qquad (1)$$

where T_{in} is the inlet air temperature, β_c is the compressor pressure ratio, γ is the specific heat ratio and η_c is the compressor isentropic efficiency.

As far as the expansion process is concerned, since the air cooling may be accompanied by condensation of water vapour, the transformation is schematically modelled according to a two-stage process [15]. The first stage is a pressure drop that, due to its high speed, is assumed to occur at a constant humidity ratio, which implies that whenever the air temperature falls below the dew point, the water vapour contained in the moist air is discharged from the turbine wheel at a sub-cooled non-equilibrium state. Under the assumption of adiabatic operation, the following first-stage outlet temperature is derived:

$$T_{\mathrm{out}} = T_{\mathrm{in}}\left[(1-\eta_{\mathrm{t}}) - \frac{\eta_{\mathrm{t}}}{\beta_{\mathrm{t}}^{(\gamma-1)/\gamma}}\right], \tag{2}$$

where T_{in} is the inlet air temperature, β_{t} is the turbine pressure ratio, and η_{t} is the turbine isentropic efficiency. The second stage is an isobaric transformation, occurring at atmospheric pressure, in which the condensation of the excess water vapour takes place up to reaching the final equilibrium saturation state at temperature T_{t} and humidity ratio x_{t}, calculated under the assumption of constant specific enthalpy of moist air by a trial-and-error procedure based on the following equations:

$$c_{\mathrm{a}}T_{\mathrm{t}} + x_{\mathrm{t}}(c_{\mathrm{v}}T_{\mathrm{t}} + \lambda_0) = c_{\mathrm{a}}T_{\mathrm{out}} + x_{\mathrm{out}}(c_{\mathrm{v}}T_{\mathrm{out}} + \lambda_0) + (x_{\mathrm{t}} - x_{\mathrm{out}})c_{\mathrm{liq}}T_{\mathrm{liq}}, \tag{3}$$

$$x_{\mathrm{t}} = 0.62198\frac{p_{\mathrm{ws}}(T_{\mathrm{t}})}{p_{\mathrm{t}} - p_{\mathrm{ws}}(T_{\mathrm{t}})}, \tag{4}$$

$$\ln p_{\mathrm{ws}}(T_{\mathrm{t}}) = \frac{C_1}{T_{\mathrm{t}}} + C_2 + C_3T_{\mathrm{t}} + C_4T_{\mathrm{t}}^2 + C_5T_{\mathrm{t}}^3 + C_6T_{\mathrm{t}}^4 + C_7\ln(T_{\mathrm{t}}), \tag{5}$$

where c_{a} and c_{v} are the specific heats at constant pressure of dry air and water vapour, respectively; λ_0 is the latent heat of vaporization of water at 0°C; T_{out} and x_{out} are the temperature and humidity ratio of moist air at the first-stage outlet (x_{out}, as mentioned, is assumed equal to x_{in}); c_{liq} is the specific heat of liquid water; T_{liq} is the temperature of the condensated liquid water, assumed equal to T_{out}; p_{ws} is the water vapour saturation pressure; p_{t} is the total pressure of moist air at the turbine outlet, i.e. atmospheric pressure; and C_1 to C_7 are the coefficients of the Hyland and Wexler equations [16].

3.2 Air-to-air heat exchangers

The transformations occurring inside the air-to-air plate heat exchangers, both conventional and wet-surface type, are simulated through a model that satisfies the following conditions: (1) steady-state operation; (2) zero wall and air thermal diffusivity in the flow directions; (3) negligible thermal resistance of the separation walls, the possible condensate film on the hot side of the heat exchanger surfaces, and the evaporating water film on the boundary surfaces of the cool airstream passages, if present; (4) negligible heat transfer between heat exchanger case and surroundings; (5) negligible radiative heat transfer between portions of the separation walls at different temperatures; (6) constant and uniform total pressure and mass flow rates for both airstreams; (7) constant and uniform specific heats at constant pressure of dry air and water vapour; (8) constant and uniform coefficients of convection heat transfer and water vapour transfer; (9) evaporating water film on the wet walls of the cool airstream passages assumed to be continuous, stationary and continuously replenished at its surface with water at the same temperature, closely approximated if the wetting water mass flow rate is negligible compared with the mass flow rate of the cool airstream.

With reference to a surface element dA, the following equations of conservation of energy and mass of water can be written:

$$G\mathrm{d}J = 2h_\mathrm{C}dA(t_\mathrm{w} - T) + 2\Delta h_\mathrm{D}dA[X_\mathrm{s}(t_\mathrm{w}) - X]\lambda(t_\mathrm{w}), \tag{6}$$

$$G\mathrm{d}X = 2\Delta h_\mathrm{D}\mathrm{d}A[X_\mathrm{s}(t_\mathrm{w}) - X], \tag{7}$$

$$g\mathrm{d}j = 2a_\mathrm{C}\mathrm{d}A(t_\mathrm{w} - t) + 2\delta a_\mathrm{D}\mathrm{d}A[x_\mathrm{s}(t_\mathrm{w}) - x]\lambda(t_\mathrm{w}), \tag{8}$$

$$g\mathrm{d}x = 2\delta a_\mathrm{D}\mathrm{d}A[x_\mathrm{s}(t_\mathrm{w}) - x], \tag{9}$$

with

$$J = c_\mathrm{a}T + X(c_\mathrm{v}T + \lambda_0), \tag{10}$$

$$j = c_\mathrm{a}t + x(c_\mathrm{v}t + \lambda_0), \tag{11}$$

where t_w is the separation wall temperature; Δ is a Boolean operator equal to 0 or 1 according to $t_\mathrm{w} > T_\mathrm{d}$ or $t_\mathrm{w} \leq T_\mathrm{d}$, T_d being the dew-point temperature of the hot airstream; δ is a Boolean operator equal to 0 or 1 according to whether the heat exchanger is a conventional type or a wet-surface type; J and j are the specific enthalpies of the hot and the cool airstreams, respectively; G and g are the mass flow rates of the hot and the cool airstreams, respectively; T and t are the temperatures of the hot and the cool airstreams, respectively; X and x are the humidity ratios of the hot and the cool airstream, respectively; h_C and a_C are the average coefficients of convection heat transfer of the hot and the cool airstreams, respectively; h_D and a_D are the average coefficients of water vapour transfer of the hot and the cool airstreams, respectively; $\lambda(t_\mathrm{w})$ is the latent heat of condensation of water at the wall temperature; $X_\mathrm{s}(t_\mathrm{w})$ and $x_\mathrm{s}(t_\mathrm{w})$ are the saturation humidity ratios of the hot and the cool airstreams, respectively, obtained from eqn (4) by the replacement of T_t and p_t with the wall temperature t_w and the total pressure of the airstream considered, respectively.

The boundary conditions to be used in solving eqns (6)–(9) are the inlet temperature and humidity ratio of each airstream, as well as the thermal flux continuity at the separation wall:

$$h_\mathrm{C}(T - t_\mathrm{w}) + \Delta h_\mathrm{D}[\mathrm{X} - X_\mathrm{s}(t_\mathrm{w})]\lambda(t_\mathrm{w}) = a_\mathrm{C}(t_\mathrm{w} - t) + \delta a_\mathrm{D}[x_\mathrm{s}(t_\mathrm{w}) - x]\lambda(t_\mathrm{w}). \tag{12}$$

With regard to the values of the average coefficients of convection h_C and a_C, reference may be made to completely 'dry' cooling and heating processes, under the assumption that convective heat transfer is not significantly affected by possible condensation or evaporation processes [17]. Thus, first-approach values for h_C and a_C may be obtained directly from the value of the overall heat transfer coefficient (U) calculated in terms of the heat exchanger effectiveness in sensible heat transfer (E) [18], which, for all the cases considered here, is related to the cool airstream, whose heat capacity rate gc at the entrance is smaller than that of the hot airstream GC:

$$E = \frac{t_\mathrm{out} - t_\mathrm{in}}{T_\mathrm{in} - t_\mathrm{in}}. \tag{13}$$

Once the value of E is assigned, the outlet temperatures of both the hot and the cool airstreams, as well as the total heat transfer rate Q, may be derived:

$$t_{\text{out}} = t_{\text{in}} + E(T_{\text{in}} - t_{\text{in}}), \tag{14}$$

$$T_{\text{out}} = T_{\text{in}} \frac{gc}{GC} E(T_{\text{in}} - t_{\text{in}}), \tag{15}$$

$$Q = gcE(T_{\text{in}} - t_{\text{in}}). \tag{16}$$

The total heat transfer rate Q may then be expressed in terms of the logarithmic mean temperature difference θ_{ml}:

$$Q = UA\theta_{\text{ml}} = UA \frac{(T_{\text{in}} - t_{\text{out}}) - (T_{\text{out}} - t_{\text{in}})}{\ln \dfrac{T_{\text{in}} - t_{\text{out}}}{T_{\text{out}} - t_{\text{in}}}}, \tag{17}$$

where A is the area of the heat transfer surface. Combining eqns (14)–(16) with eqn (17), the following expression for the overall heat transfer coefficient U may be derived:

$$U = \frac{1}{A} \cdot \frac{gc}{1 - \dfrac{gc}{GC}} \cdot \ln \frac{1 - E\dfrac{gc}{GC}}{1 - E}, \tag{18}$$

in which, by neglecting the thermal resistance of the separation wall, the condensate film on the boundary surfaces of the hot airstream passages, if present, and the evaporating water film on the boundary surfaces of the cool airstream passages, if the heat exchanger is a wet-surface type, U may be expressed in terms of the average coefficients of convection of the hot and the cool airstreams:

$$U = \frac{1}{\dfrac{1}{h_{\text{C}}} + \dfrac{1}{\alpha_{\text{C}}}}. \tag{19}$$

It then follows:

$$\frac{1}{\dfrac{1}{\alpha_{\text{C}}}\left(\dfrac{\alpha_{\text{C}}}{h_{\text{C}}} + 1\right)} = \frac{1}{A} gB = \frac{1}{A} GRB \tag{20}$$

with:

$$R = \frac{g}{G}, \tag{21}$$

$$B = \frac{c}{1 - R\dfrac{c}{C}} \cdot \ln \frac{1 - ER\dfrac{c}{C}}{1 - E}. \tag{22}$$

Taking into account the more usual values for the plate spacing of air-to-air heat exchangers (assumed to be of the order of 10^{-2}–10^{-3} m) and the air mean velocity (assumed to be of the order of 1–5 m/s), in most situations the flow regime of both airstreams is laminar, which seems to be a cautious assumption for a first-approach study. Therefore, since the overall Nusselt number of both airstreams may be considered as proportional to $Re^{0.33}$ [19], when further assumptions of the same distance between the plates for the passage of both airstreams and not too different values of their physical properties are made, it follows that:

$$\frac{a_{\mathrm{C}}}{h_{\mathrm{C}}} = \frac{Nu_{\mathrm{cool}}}{Nu_{\mathrm{hot}}} = \frac{(Re_{\mathrm{cool}})^{0.33}}{(Re_{\mathrm{hot}})^{0.33}} = (g/G)^{0.33} = R^{0.33}. \tag{23}$$

Hence,

$$h_{\mathrm{C}} = U\frac{1+(g/G)^{0.33}}{(g/G)^{0.33}} = \frac{1}{A}GB\frac{1+R^{0.33}}{R^{0.33}}, \tag{24}$$

$$a_{\mathrm{C}} = U\left[1+(g/G)^{0.33}\right] = \frac{1}{A}GB(1+R^{0.33}). \tag{25}$$

Finally, the average coefficients of water vapour transfer are evaluated by the Lewis relation:

$$h_{\mathrm{D}} = \frac{h_{\mathrm{C}}}{C} = \frac{1}{A}\cdot\frac{GB}{C}\cdot\frac{1+R^{0.33}}{R^{0.33}}, \tag{26}$$

$$a_{\mathrm{D}} = \frac{a_{\mathrm{C}}}{c} = \frac{1}{A}\cdot\frac{gB}{c}(1+R^{0.33}). \tag{27}$$

According to eqns (24)–(27), the conservation equations (6)–(9) and relation (12) become:

$$\mathrm{d}J = 2BR\frac{1+R^{0.33}}{R^{0.33}}\left\{(t_{\mathrm{w}}-T)+\frac{\Delta}{C}[X_{\mathrm{s}}(t_{\mathrm{w}})-X]\lambda(t_{\mathrm{w}})\right\}\frac{\mathrm{d}A}{A}, \tag{28}$$

$$\mathrm{d}X = 2BR\frac{1+R^{0.33}}{R^{0.33}}\cdot\frac{\Delta}{C}[X_{\mathrm{s}}(t_{\mathrm{w}})-X]\frac{\mathrm{d}A}{A}, \tag{29}$$

$$\mathrm{d}J = 2B(1+R^{0.33})\left\{(t_{\mathrm{w}}-t)+\frac{\delta}{c}[x_{\mathrm{s}}(t_{\mathrm{w}})-x]\lambda(t_{\mathrm{w}})\right\}\frac{\mathrm{d}A}{A}, \tag{30}$$

$$\mathrm{d}x = 2B(1+R^{0.33})\frac{\delta}{c}[x_{\mathrm{s}}(t_{\mathrm{w}})-x]\frac{\mathrm{d}A}{A}, \tag{31}$$

$$(T-t_{\mathrm{w}})+\frac{\Delta}{C}[X-X_{\mathrm{s}}(t_{\mathrm{w}})]\lambda(t_{\mathrm{w}}) = R^{0.33}\left\{(t_{\mathrm{w}}-t)+\frac{\delta}{c}[x_{\mathrm{s}}(t_{\mathrm{w}})-x]\lambda(t_{\mathrm{w}})\right\}. \tag{32}$$

Finite-difference equations are derived by integrating eqns (28)–(31) over a discrete surface element of the heat exchanger, and solved iteratively by taking into account the inlet boundary conditions as well as eqn (32). Uniform mesh spacing is employed, with a minimum number of 50 subdivisions of the heat transfer surface, which compromises between computational times and simulation accuracy, as determined through a series of preliminary numerical tests. Under-relaxation is used to ensure convergence. The solution is considered to be fully converged when percentage changes of both temperature and humidity ratio at each location from iteration to iteration are smaller than a prescribed value, i.e. 10^{-5}. With regard to the value of the mass flow rate ratio R, for heat exchangers HE1–HE3, R is assumed equal to unity. In contrast, for heat exchanger HE4 the first approximation value of $R \leq 1$ is assumed and a trial-and-error procedure is followed in order to calculate the mass flow rate ratio R which corresponds to the achievement of the assigned value of the supply air temperature t_S.

3.3 Air washers

The temperature and humidity ratio of the airstreams at the exit of the air washers are calculated through the saturation effectiveness ε [20] under the assumption of the outlet state being at practically the same specific enthalpy of the inlet state:

$$\varepsilon = \frac{T_{in} - T_{out}}{T_{in} - T_{wet}}. \tag{33}$$

Hence,

$$T_{out} = T_{in} - \varepsilon(T_{in} - T_{wet}), \tag{34}$$

$$x_{out} = \frac{1}{c_v T_{out} + \lambda_0}\left[c_a(T_{in} - T_{out}) + x_{in}(c_v T_{in} + \lambda_0)\right], \tag{35}$$

where T_{in} and T_{out} are the inlet and outlet dry-bulb temperatures, respectively; x_{in} and x_{out} are the inlet and outlet air humidity ratios, respectively; and T_{wet} is the wet-bulb temperature of air at the inlet, whose value may be calculated under the assumption of saturation occurring at practically constant specific enthalpy through a trial-and-error procedure based on eqns (3)–(5) by replacing subscripts 't' and 'out' with 'wet' and 'in', respectively, and by neglecting the third term on the right-hand side of eqn (3).

4 NUMERICAL SIMULATIONS

The analysis of the cooling performance of any HVAC system discussed is conducted under the assumption that the mass flow through the heat exchangers occurs with negligible frictional losses, which corresponds to the assumption that the compressor and expander pressure ratios are the same.

Simulations are performed with reference to indoor air conditions of 25°C and 50% RH, for different values of the outdoor air temperature t_E in the range between 25 and 45°C, the outdoor air humidity ratio x_E in the range between 0.015 and 0.030 kg/kg-dry-air, the supply air temperature t_S in the range between 12 and 25°C, the effectiveness in sensible heat transfer of the heat exchangers

E in the range between 0.6 and 0.9, and the compressor and turbine isentropic efficiency η in the range between 0.7 and 0.9.

5 RESULTS AND DISCUSSION

For each situation analysed, the pressure ratio β required for cooling and dehumidification of outdoor air up to reaching the moisture content assigned for the supply air, i.e. 0.009 kg/kg-dry-air, which is the humidity ratio relevant to 25°C at approximately 45% RH, is calculated iteratively. The corresponding cooling performance ξ of the HVAC system, defined as the ratio of the heat q_{ref} removed from the outdoor air to be supplied to the indoor ambient, and the net work input w_{net}, given by the difference between the compressor work input w_{c} and the turbine work output w_{t}, is then derived:

$$\xi = \frac{q_{\mathrm{ref}}}{w_{\mathrm{net}}} = \frac{q_{\mathrm{ref}}}{w_{\mathrm{c}} - w_{\mathrm{t}}}. \tag{36}$$

In eqn (36), q_{ref} is calculated by the specific enthalpy difference between the states of outdoor air and saturated supply air at the introduction humidity ratio of 0.009 kg/kg-dry-air. Also w_{c} and w_{t} are calculated in terms of specific enthalpy changes, under the assumption of steady-flow adiabatic operation of the turbomachinery, and negligible effects of kinetic and potential energies.

The results obtained are described and discussed in the following three subsections.

5.1 Conventional HVAC systems

Typical distributions of ξ for the four conventional configurations CS1–CS4 are plotted in Fig. 11 versus the outdoor air temperature t_{E} for $x_{\mathrm{E}} = 0.015$ kg/kg-dry-air, $E = 0.75$ and $\eta = 0.85$, and in Fig. 12 versus the outdoor air humidity ratio x_{E} for $t_{\mathrm{E}} = 35$°C, $E = 0.75$ and $\eta = 0.85$.

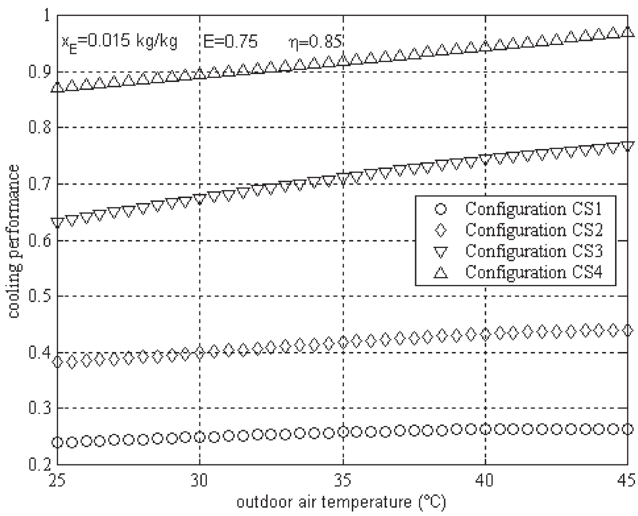

Figure 11: Distributions of ξ vs t_{E} for configurations CS1–CS4.

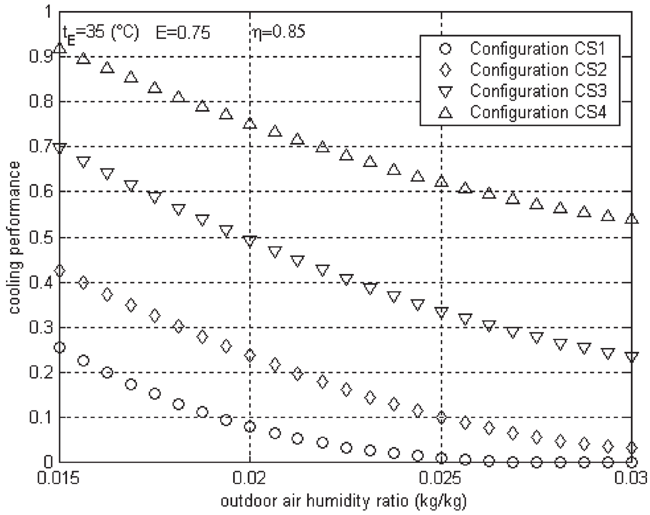

Figure 12: Distributions of ξ vs x_E for configurations CS1–CS4.

It may be noticed that for any conventional HVAC system, ξ decreases with increasing outdoor air humidity ratio, which is due to the increase in the amount of heat q_{ref} which has to be removed from outdoor air. In fact, once t_E, E and η are assigned, the higher is the value of q_{ref}, the lower must be the temperature of the expanded cool air at the inlet of heat exchanger HEC. This may be obtained only by increasing the pressure ratio β, with a consequent very pronounced increase in the net work input w_{net} required by the air-cycle machine. In contrast, ξ keeps nearly constant with increasing t_E, owing to the corresponding increase in the amount of heat exchanged inside HEC.

In addition, it may be observed that ξ increases as the number of heat exchangers decreases, i.e. passing from configuration CS1 to configuration CS4. However, the cooling performance of the most efficient configuration, namely ξ(CS4), is actually too small in comparison with the values typical for traditional HVAC systems served by vapour-compression refrigerating units, which reflects the present limited use of air-cycle machines for air-conditioning purposes.

5.2 Basic integrated HVAC systems

Once configuration CS4 is assumed as the reference conventional HVAC system, increases in the cooling performance up to 25% may be obtained by the adoption of the basic integrated HVAC systems BIS1 and BIS2, e.g. as shown in Fig. 13, where the distributions of ξ(BIS1)/ξ(CS4) and ξ(BIS2)/ξ(CS4) are plotted versus the outdoor air temperature t_E for x_E = 0.015 kg/kg-dry-air, E = 0.75 and η = 0.85.

In practice, such non-negligible percentage increases for ξ are of little interest, as the cooling performance of the system remains of the order of unity, which is still too low. In addition, it seems worth pointing out that if the values assumed for E and η are 0.7 and 0.8, instead of 0.75 and 0.85, respectively, a remarkable decrease of ξ from a mean value of 1.05 to a mean value of 0.7 is observed. Moreover, if the outdoor air humidity ratio is taken equal to 0.0175 kg/kg-dry-air instead of 0.015 kg/kg-dry-air, a further decrease of ξ to a mean value of 0.575 occurs.

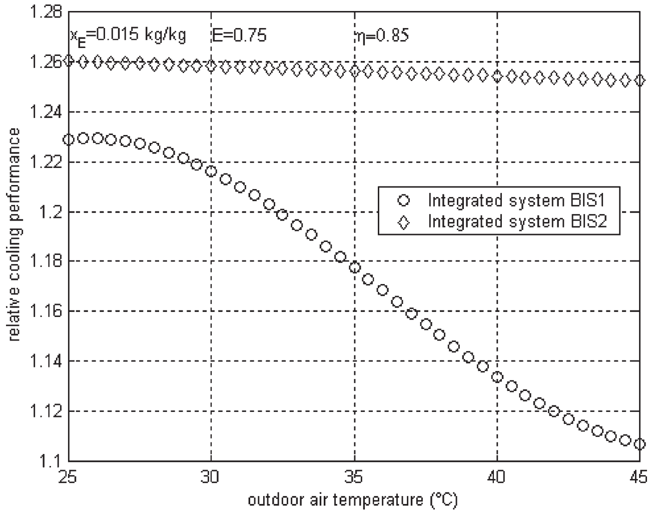

Figure 13: Distributions of ξ(BIS1)/ξ(CS4) and ξ(BIS2)/ξ(CS4) vs t_E.

Indeed, since very high values of the energetic efficiencies of both the heat exchangers and the turbomachinery are unrealistic, at least from the practical and economic points of view, and very low values of the outdoor air humidity ratio are encountered not so often, the aforementioned examples help to understand that the shift from basic to enhanced integrated HVAC configurations becomes absolutely mandatory.

5.3 Enhanced integrated HVAC systems

Typical distributions of ξ for the three configurations EIS1, EIS2, and EIS3, are reported:

1. in Fig. 14, versus the outdoor air temperature t_E for x_E = 0.0175 kg/kg-dry-air, E = 0.7, η = 0.8 and different values of the supply air temperature t_S;
2. in Fig. 15, versus the outdoor air humidity ratio x_E for t_E = 35°C, E = 0.7, η = 0.8 and different values of the supply air temperature t_S;
3. in Fig. 16, versus the turbomachinery isentropic efficiency η for t_E = 35°C, x_E = 0.0175 kg/kg-dry-air, t_S = 20°C and different values of the effectiveness in sensible heat transfer of the heat exchangers E.

It may be observed that the cooling performance ξ of any integrated HVAC system analysed increases as the outdoor air temperature increases. In fact, increases in t_E imply increases in Δq_{ref} and Δw_{net} in both the amount of heat which has to be removed from outdoor air and the net work input which has to be transferred to the air-cycle machine, respectively. On the other hand, increases in t_E imply larger heat transfer rates inside HE1, and in many cases also inside HE2 (due to the increase in temperature difference between the airstreams at the inlet), which help to curb Δw_{net} with respect to Δq_{ref}, with non-negligible increases in the cooling performance. In contrast, ξ decreases as the outdoor air humidity ratio increases. In fact, increases in x_E result in values of Δw_{net} proportionally

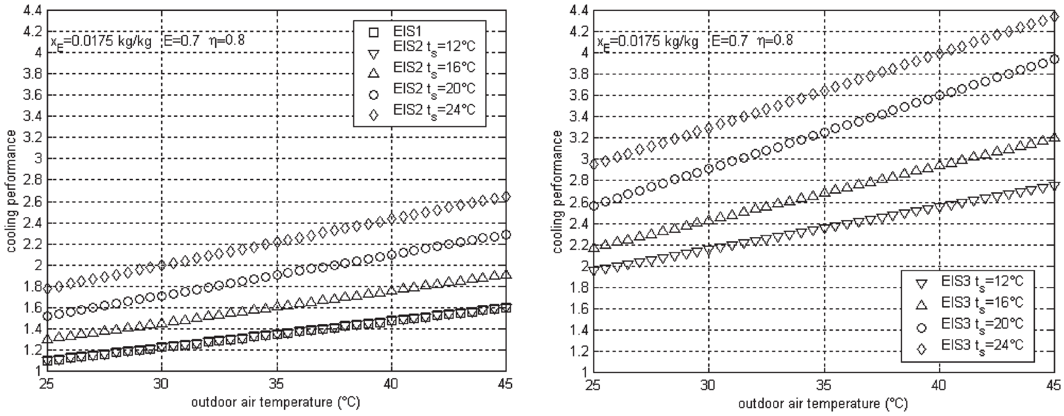

Figure 14: Distributions of ξ vs t_E for configurations EIS1–EIS3.

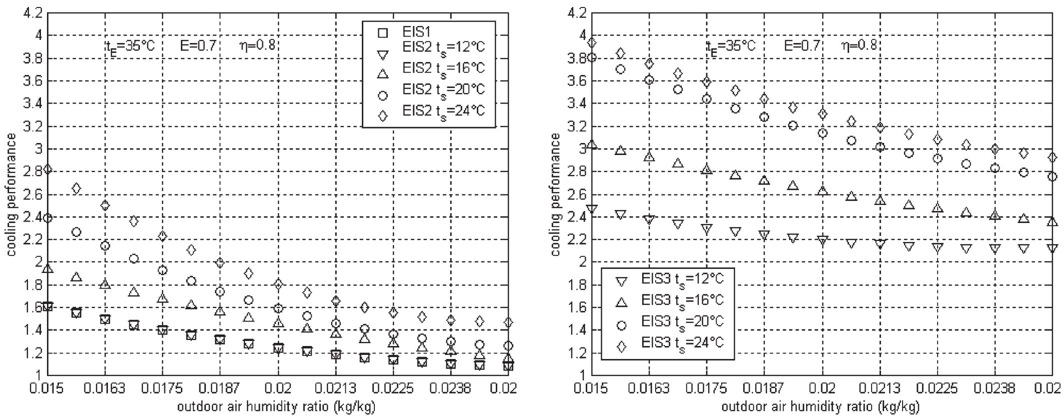

Figure 15: Distributions of ξ vs x_E for configurations EIS1–EIS3.

larger than those of Δq_{ref}, owing to the reduced heat transfer rates inside HE1 and HE2. Of course, these are only first-approach explanations, as the performance of each component of the system depends on both the climatic conditions and the performance of any other component, which makes it impossible to bring forth a linear analysis.

Moreover, for both systems EIS2 and EIS3, ξ increases with increasing supply air temperature t_S, owing to the increase in the flow rate of expanded cool air which passes through heat exchanger HE4. Finally, for any configuration analysed, the cooling performance ξ increases with increasing the heat transfer effectiveness E of heat exchangers and the isentropic efficiency η of turbomachinery.

As far as the required pressure ratio is concerned, its distributions have trends which, in line with principle, are just the opposite of those observed for the cooling performance. In fact, β increases as the isentropic efficiency η of turbomachinery, the effectiveness E of heat exchangers, and the supply air temperature t_S decreases, and as the outdoor air humidity ratio x_E increases. The only exception is represented by the outdoor air temperature t_E, whose changes do not have significant effects on β.

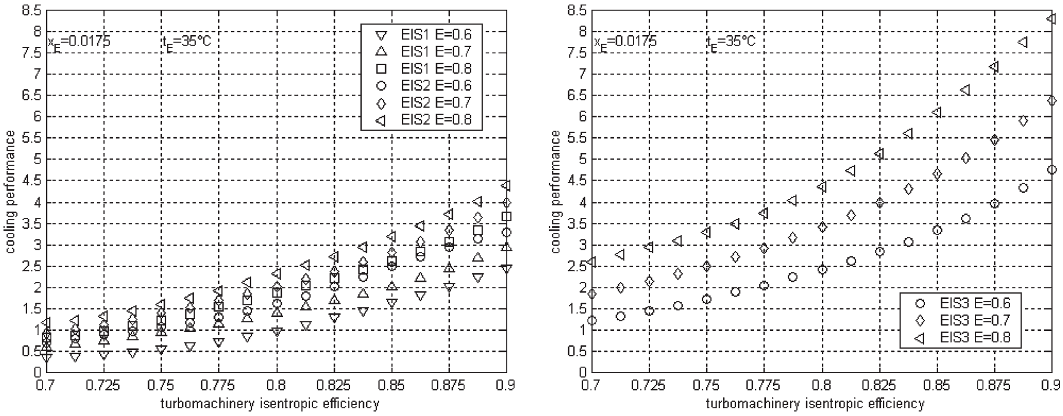

Figure 16: Distributions of ξ vs η for configurations EIS1–EIS3.

Typical values of β are in the range between 1.2 and 3, the lower values being typical for the enhanced configurations EIS2 and EIS3.

It is worth noticing that the cooling performance of configuration EIS3 may reach values up to twice and thrice those typical for configurations EIS2 and EIS1, respectively. More important, for hot and dry inland climates (e.g. as is the case in many US states and countries of the Middle East and the South Mediterranean basin), and also for temperate climates (e.g. as is the case in many countries of the North Mediterranean basin), values of the cooling performance of the same order as those typical for traditional HVAC systems served by vapour-compression refrigerating units are obtained (i.e. in the range between 3 and 4), which is the main result of the whole investigation.

As expected, the best values of cooling performance are those obtained for the highest supply air temperatures considered. This suggests that the use of the enhanced integrated HVAC systems is of great interest whenever consistent rates of air changes per hour are required, which necessarily implies small temperature differences between indoor air and supply air (e.g. as in the case of the operating rooms or critical care areas in health facilities). In this regard, in hospital applications or when possible cross contaminations between the airstreams must be avoided, the replacement of any air-to-air heat exchanger with a double-coil equipment (i.e. an equipment consisting of a pair of extended surface, finned-tube coils placed in the two airstreams and connected in a closed loop via counterflow piping) may then be considered. In such cases, as the heat transfer effectiveness of double-coil systems is generally smaller than that of the direct air-to-air heat exchangers, larger heat transfer surfaces should be adopted, and the flow rate of the intermediate fluid has to be defined according to optimization procedures [21].

6 CONCLUSIONS

The cooling performance of new air-conditioning systems based on the reversed Brayton cycle has been calculated through a specifically developed computer code, in order to evaluate their actual applicability. Such systems, which we have named ‘integrated HVAC systems’, combine the roles traditionally played separately by the chiller and the air handler, as expanded cool air is directly supplied to the indoor ambient for its environmental control.

Several different configurations of such integrated systems have been proposed and discussed. For each of them, numerical simulations have been carried out for a wide variety of psychrometric states of both outdoor air and supply air, so as to cover different summer climatic conditions, and for different values of the efficiency of both the heat exchangers and the turbomachinery.

The main results obtained for the most advanced configurations proposed may be summarized as follows:

1. The cooling performance, defined as the ratio between the heat to be removed from outdoor air and the net work input required by the air-cycle machine, increases as the temperatures of outdoor air and supply air increase, the humidity ratio of outdoor air decreases, and the efficiencies of heat exchangers and turbomachinery increase.
2. For hot and dry climates, as well as for temperate climates, values of the cooling performance of the same order as those typical for traditional HVAC systems served by vapour-compression refrigerating units may be obtained;
3. High supply air temperatures result in good cooling performance, which means that whenever high rates of air changes per hour are required, such integrated systems are well applicable.

These very-encouraging first-approach results are to be verified through measurements that will be executed on an experimental set-up, whose design and construction is in progress.

NOMENCLATURE

A	heat transfer surface area
c	specific heat at constant pressure
E	effectiveness in sensible heat transfer of heat exchangers
G	mass flow rate of the hot airstream
g	mass flow rate of the cool airstream
h_C	average coefficient of convection heat transfer of the hot airstream
h_D	average coefficient of water vapour transfer of the hot airstream
J	specific enthalpy of the hot airstream
j	specific enthalpy of the cool airstream
Nu	Nusselt number
p	pressure
Q	total heat transfer rate
q	heat per unit mass
R	cool-to-hot mass flow rate ratio
Re	Reynolds number
T	temperature, temperature of the hot airstream
t	temperature of the cool airstream
U	overall heat transfer coefficient
X	humidity ratio of the hot airstream
x	humidity ratio, humidity ratio of the cool airstream
w	work per unit mass
α_C	average coefficient of convection heat transfer of the cool airstream
α_D	average coefficient of water vapour transfer of the cool airstream
β	pressure ratio
Δ, δ	boolean operators

ε	saturation effectiveness of air washers
γ	specific heat ratio
η	isentropic efficiency
λ	latent heat of vaporization/condensation of water
θ_{ml}	logarithmic mean temperature difference
ξ	cooling performance of the HVAC system

Subscripts

a	dry air
c	compressor
cool	cool airstream
d	dew point
E	external air
hot	hot airstream
in	inlet
liq	liquid water
net	net input
out	outlet
ref	refrigeration
S	supply air
s	saturation
t	turbine, total
v	water vapour
w	separation wall
wet	wet bulb
ws	water vapour at saturation
0	at 0°C

REFERENCES

[1] Fantini, L. & Nannei, E., Sull'utilizzazione di un ciclo inverso a gas in macchine ad effetto frigorigeno, prima parte. *Il Freddo*, 2/91, p. 175, 1991.

[2] Mattarolo, L., Tecnologia del freddo e impatto ambientale. *Il Freddo*, 6/94, p. 495, 1994.

[3] Lorentzen, G., The use of natural refrigerants: a complete solution to the CFC/HCFC predicament. *Int. J. Refrig.*, **18(3)**, pp. 190–197, 1995.

[4] Riffat, S.B., Afonso, C.F., Oliveira, A.C. & Reay, D.A., Natural refrigerants for refrigeration and air-conditioning systems. *Appl. Therm. Eng.*, **17(1)**, pp. 33–42, 1997.

[5] Kruse, H., L'impiego dei fluidi naturali. *Il Freddo*, 1/97, p. 41, 1997.

[6] Gigiel, A., De Chauveron, S. & Fitt, P., Air as a replacement for CFC refrigerants. *Proposals for the Generation and Use of Refrigeration in the 21st Century*, Buenos Aires, Argentina, IIR/IIF edn, pp. 83–92, 1992.

[7] ASHRAE, Air-cycle equipment (Chapter 14). *1988 ASHRAE Handbook: Equipment*, ASHRAE: Atlanta, GA, 1988.

[8] Cappelli D'Orazio, M., Cianfrini, C. & Corcione, M., An air-conditioning system based on the reverse Joule-Brayton cycle. *Int. J. Heat Technol.*, **18(2)**, pp. 91–100, 2000.

[9] Cappelli D'Orazio, M., Cianfrini, C., Corcione, M. & Moncada, G., Developments of reverse open air-cycle systems for air conditioning terrestrial applications. *Proc. of the 7th Rehva World Congress Clima 2000*, Naples, Italy, 2001.

[10] Pescod, D., A heat exchanger for energy saving in an air conditioning plant. *ASHRAE Trans.*, **85**, pp. 238–251, 1979.

[11] Maclaine-Cross, I.L. & Banks, P.J., A general theory of wet surface heat exchangers and its application to regenerative evaporative cooling. *J. Heat Transfer*, **103**, pp. 579–585, 1981.

[12] Dumas, A. & Piva, S., Analisi di scambiatori statici aria-aria con fenomeni di condensazione ed evaporazione. *CDA*, 3-88, p. 389, 1988.

[13] Dumas, A. & Corradini, E., Presenza di un velo liquido di acqua sulle superfici di uno scambiatore aria-aria. *CDA*, 9-96, p. 1012, 1996.

[14] Corcione, M., A wet surface three-fluid type heat exchanger for energy recovery in air-conditioning plants. *Int. J. Heat Technol.*, **19(1)**, pp. 85–94, 2001.

[15] Fantini, L. & Nannei, E., Sull'utilizzazione di un ciclo inverso a gas in macchine ad effetto frigorigeno, seconda parte. *Il Freddo*, **2**/91, p. 277, 1991.

[16] Hyland, R.W. & Wexler, A., Formulations of the thermodynamic properties of the saturated phases of H_2O from 173.15 K to 473.15 K. *ASHRAE Trans.*, **89**, pp. 500–519, 1983.

[17] Smolsky, B.M. & Sergeev, G.T., Heat and mass transfer with liquid evaporation. *Int. J. Heat Mass Transfer*, **5(11)**, pp. 1011–1021, 1962.

[18] ASHRAE, Air-to-air energy-recovery equipment (Chapter 34). *1988 ASHRAE Handbook: Equipment*, ASHRAE: Atlanta, GA, 1988.

[19] Hausen, H., Darstellung des Warmeuberganges in Rohren durch verallgemeinerte Potenz-beziehungen. *Z. VDI*, Beihefte Verfahrenstechink, **4**, p. 91, 1943.

[20] ASHRAE, Evaporative air-cooling equipment (Chapter 4). *1988 ASHRAE Handbook: Equipment*, ASHRAE: Atlanta, GA, 1988.

[21] Cappelli D'Orazio, M., Cianfrini, C., Corcione, M. & Fontana, D.M., Optimal design and energetic performance of double finned-tube coil energy-recuperators. *Int. J. Heat Technol.*, **19(1)**, pp. 11–22, 2001.